# Analysis of power devices breakdown behaviour by ion beam and electron beam induced charge microscopy

R. Siemieniec [(1)], A. Pugatschow [(1)], C. Geissler [(2)], H.-J. Schulze [(3)], F.-J. Niedernostheide [(3)], R. Heiderhoff [(4)] and L.J. Balk [(4)]

[(1)] Infineon Technologies Austria AG, Villach, Austria
[(2)] Infineon Technologies AG, Regensburg, Germany
[(3)] Infineon Technologies AG, Munich, Germany
[(4)] Bergische Universität Wuppertal, Wuppertal, Germany

## *Abstract*

*The development of appropriate edge termination structures is a challenging task for all kinds of different vertical power semiconductors such as high-voltage diodes, IGBTs or especially compensation devices. Ion-beam induced charge microscopy and electron-beam induced charge microscopy are reliable tools for imaging of space-charge regions and detection of electric-field enhancements inside of power devices. The usefulness of these methods is shown for the example of high-voltage power diodes and low-voltage power MOSFET. Advantages and limitations of the measurement techniques are discussed.*

**Keywords:** Diode, MOSFET, EBIC, IBIC, Measurement, Electric Field

## INTRODUCTION

Beam-induced current methods allow the acquisition of local electrical device behaviour, such as expansion of the space-charge region. These methods generate excess charge carriers within a small part of the device by a focused ion or electron beam. These generated carriers can be detected and the analysis of these data offers a powerful tool for the investigation of electric field strengths and distributions as well as for the evaluation of the space-charge region in power devices under stationary and dynamic conditions.

IBIC (Ion Beam Induced Charge) microscopy [1] is well-established for the analysis of microelectronic structures such as integrated circuits [2], light-emitting diodes [3], CMOS transistors [4] and radiation detectors [5], and also several kinds of power devices [6]. Light ions exhibit a small lateral spread of about 6 µm in diameter when structures about 100 µm deep are analyzed. Ions lose most of their energy close to the end of the generation volume. Thus, IBIC microscopy is most sensitive in the region close to the end of the ion range which enables a depth resolution by using different ion energies.

EBIC (Electron Beam Induced Current) measurements have been used to observe space-charge regions [7] as well as electric-field distributions [8,9] of silicon and silicon-carbide high-power high-voltage devices under static and dynamic biasing conditions. EBIC maps allow a low spatial resolution in the range of 1 µm (depending on the examined depth), thus enabling the analysis of smaller device structures such as field-plate trench MOSFETs [10]. The energy of the electron beam controls the penetration depth and needs to be adjusted in accordance with the passivation layer thickness.

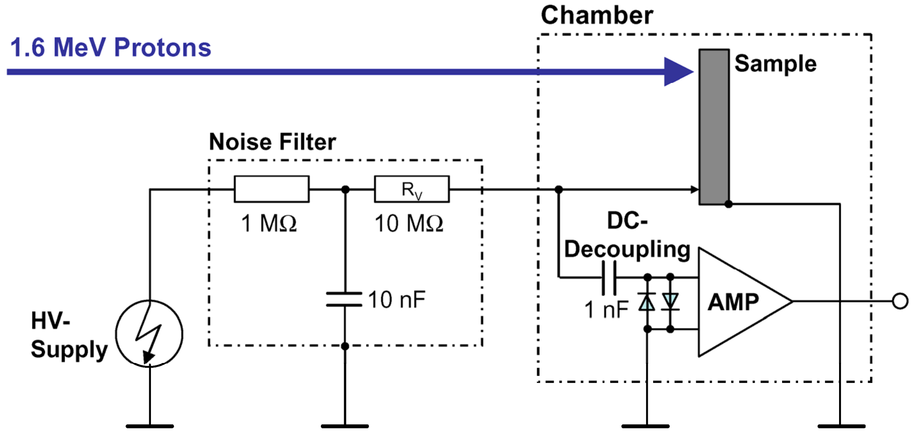


Fig. 1: Setup for stationary IBIC measurements on high-voltage power devices

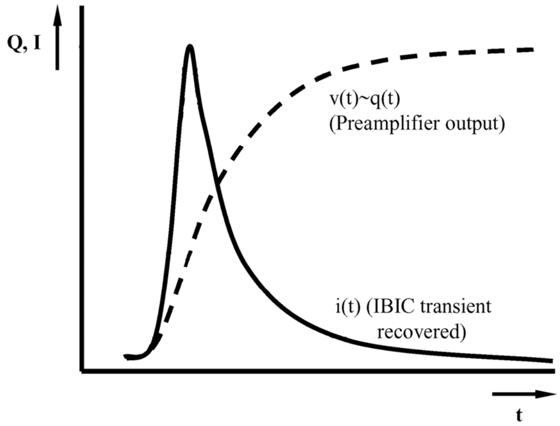


Fig. 2: Transient of collected charge q(t) and derived current transient i(t) of an IBIC signal [11]

## MEASUREMENT SETUP

### IBIC Microscopy

Fig. 1 shows the schematic setup that was used for stationary IBIC measurements on high-voltage devices. Each ion generates carriers within a space-charge region which are separated due to internal electric fields provided by a pn-junction or a Schottky contact. A charge-sensitive preamplifier detects the generated charge. The generated current pulses are integrated due to noise-reduction reasons and translated into a voltage pulse which increase in time and finally reaches a saturation value as shown in Fig. 2. This value is proportional to the number of charges separated in the space-charge region.

The overall collected charge itself remains almost constant even if the electric field strength varies inside the space-charge region. However, the shape of the induced current transient does depend on the electric field distribution. Consequently, a time-resolved measurement can be done by differentiating the previously recorded voltage pulse. The result is the recovered current pulse $i(t) = dq/dt$ as shown in Fig. 2. This current pulse is characterized by a rise time, a pulse duration time and a peak current value. Due to the dependence of the drift velocity on the electric field strength, all these parameters depend on the varying strength of the electric field and can therefore be used to analyse the distribution of the electric field [11]. If extremely high electric fields are present, the overall charge (the area under the curve) varies due to the charge multiplication by avalanche carrier generation. The acquisition and analysis of the collected data are done by employing a state-of-the-art data acquisition system.

Although most devices investigated by means of IBIC microscopy are still useable after the measurements, the IBIC method is not without influence on the devices under test. The ion beam introduces damages to the crystal structure of the semiconductor and deposits impurities due to the ion beam.

### EBIC Microscopy

As carrier distributions of high-voltage devices can be significantly different under stationary and dynamic conditions, time-resolved measurements are essential to analyse the device behaviour. A problem arises due to the fact that the switching transient has amplitudes of several Amperes or more while the EBIC signal is in the range of just some microamperes. To enable the separation of the EBIC signal from the switching transient, a Wheatstone bridge with two identical diodes (one being the device under test) is used as shown in Fig. 3. The Wheatstone bridge is driven by the switching circuit, and the two impedances in the circuit are carefully adjusted to reduce the difference in the voltage drops to a minimum value. Only the device under test is exposed to the electron beam, generating a voltage drop over the corresponding impedance and therefore a voltage difference which is fed to the amplifier. To achieve a good signal-to-noise ratio during the measurements, a lock-in amplifier with the same reference frequency as used to trigger the electric pulse collects the EBIC signal sensitive to phase and frequency [9]. During the measurement a focused and periodically pulsed electron beam is scanned over the surface of the device under test. Charge-carrier pairs are generated by primary electrons and separated in space-

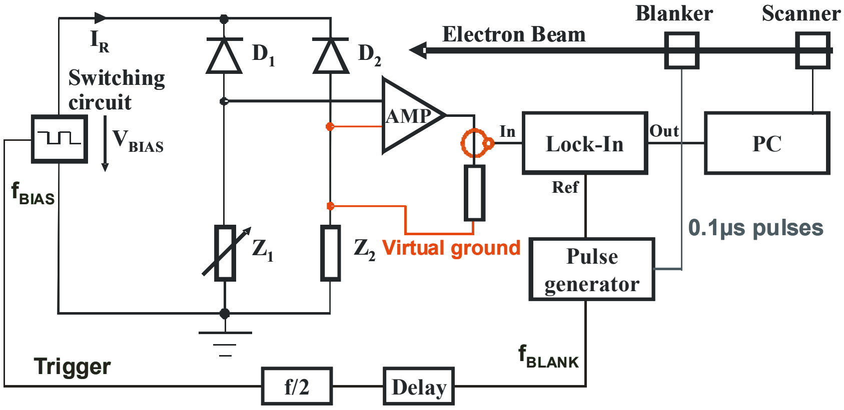


Fig. 3: Setup for dynamic EBIC measurements on high-voltage diodes [9]

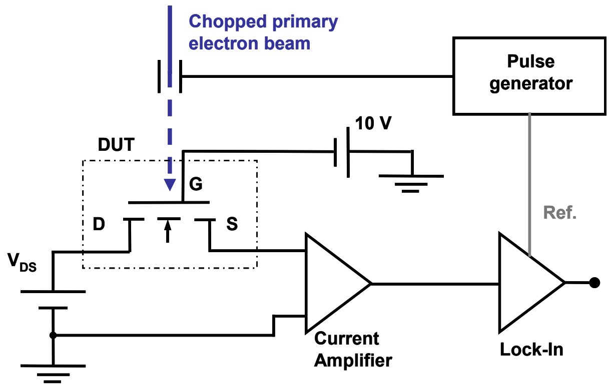


Fig. 4: Setup used for stationary EBIC measurements on power MOSFETs

charge regions due to the electric field, resulting in a current that is used to generate the EBIC signal. As in the case of IBIC microscopy, the induced current can be related to the electric field strength and time-resolved measurements are possible. For an investigation of the evolution of the electric field in time, the diode must be switched and EBIC measurements must be performed at different points in time during the switching process; thus the electron beam must be blanked in phase with the switching of the device under test. Even if the switching transient is suppressed by the measurement circuit, the signal-to-noise ratio is lower compared to stationary EBIC microscopy.

The EBIC investigations of steady-state biased MOSFET structures were performed inside a scanning electron microscope. Here, a chopped electron beam with a primary electron energy of 25 keV generated electron hole pairs inside the active area and the termination structure of the field effect transistor. The free charge carriers were separated due to internally or externally applied electric fields, which led to a current flow. The current was measured at the source contact of the transistor using a current amplifier. Again, a lock-in amplifier was employed to achieve a good signal-to-noise ratio during the measurement. By scanning the electron beam over the device, an area of approximately 130 x 130 $\mu m^2$ was imaged. The spatial EBIC resolution for these measurements was determined to be 1.2 µm. The gate of the n-channel power MOSFET was statically biased with a negative voltage $V_G = -10$ V in order to ensure that the device remained in the blocking state. The drain-to-source voltage was increased stepwise from 0 V to the voltage where field enhancement occurs, while the EBIC micrographs were recorded. Fig. 4 shows the measurement configuration described above.

## INVESTIGATED DEVICES AND RESULTS

### High-voltage power diode

**Device Structure.** Edge termination structures of several discrete power diodes rated to different blocking voltages were investigated. The edge termination structure surrounding the active device area consisted of one or more field-rings, where the number of rings depends on the voltage rating. The basic structure is shown in Fig. 5. Here, the dotted square indicates the investigated part of the device.

**IBIC Microscopy.** The investigated device was rated for a voltage of 1200 V. IBIC measurements were performed for different reverse voltages. The ion energy was adjusted in order to investigate the device surface. All images were normalized to the measurement with the maximum reverse voltage of 1250 V. Therefore, a comparison of the measurements is possible. Fig. 6 shows the amount of collected charge as the main pn-

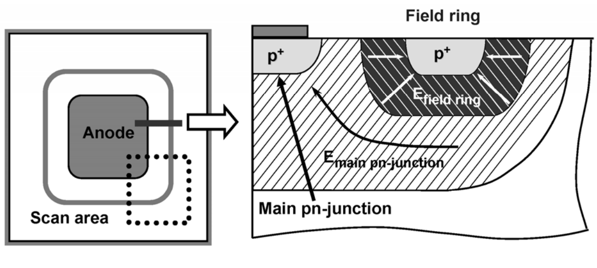


Fig. 5: Schematic drawing of the field-ring junction termination structure of the high-voltage diode

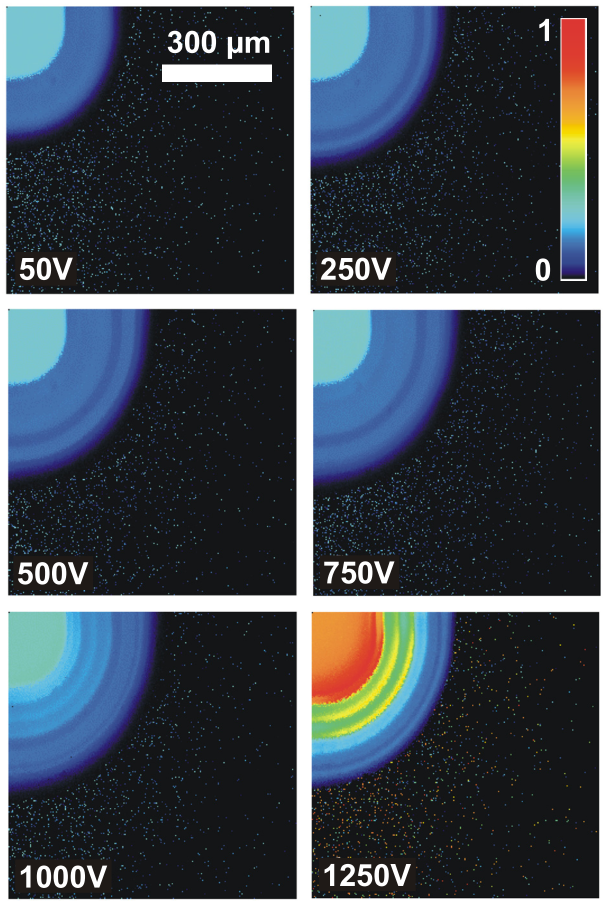


Fig. 6: IBIC maps of the 1200 V diode for different blocking voltages

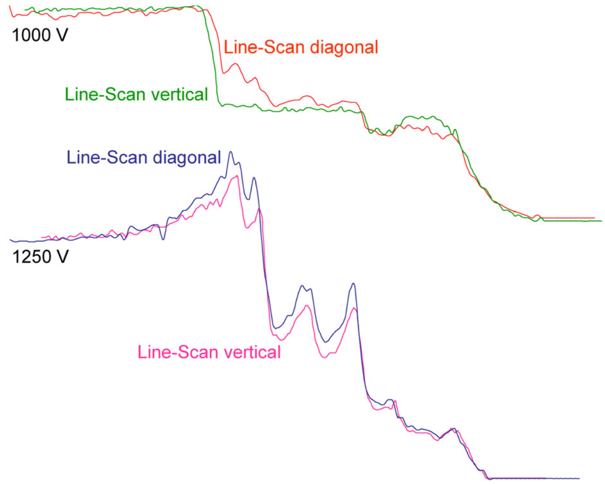


Fig. 7: IBIC line-scans for the 1200 V diode

junction extends with increasing reverse voltage. The detected value of the charge in the central section of the device remains almost constant as long as no breakdown occurs. Exceeding the rated blocking voltage triggers avalanche generation of carriers which increases the total charge. Furthermore, the measurement shows larger values at the corner where the strength of the electric field is increased. This effect cannot be seen at lower voltages. Line-scans are better suited to indicate the spatial location of avalanche multiplication of carriers. Fig. 7 shows line-scans for two different voltages in the vertical and diagonal directions through the investigated part of the device according to Fig. 5. The line-scan at a voltage of 1250 V clearly indicates the increased electrical field in the diagonal direction along the edge of the device compared to the vertical direction. This field enhancement in the outer corner should be avoided by appropriate measures to minimize reliability risks.

**EBIC Microscopy.** By means of EBIC measurements, the switching behaviour of another power diode rated for 800 V was investigated. The measurements were performed while the device was turned-off to observe dynamic effects. Fig. 8 shows the measured diode voltage and current transients. Exemplary EBIC maps are shown at four times while turning-off of the diode:

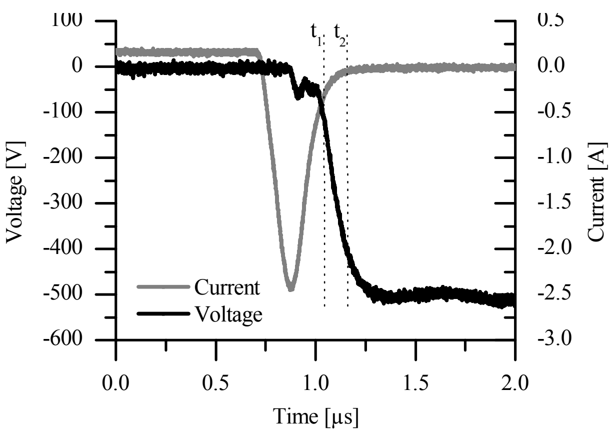


Fig. 8: Current and voltage waveform of turn-off of a 800 V power diode

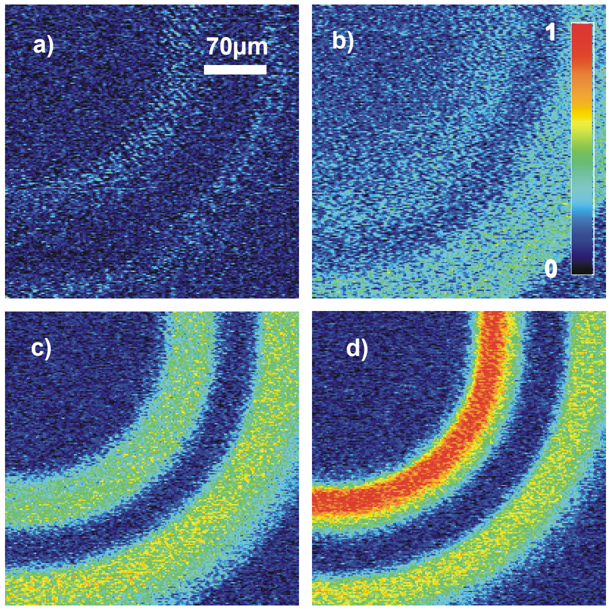


Fig. 9: EBIC maps for different phases of power diode turn-off
a) on-state of device
b),c) expansion of space-charge region (refer to $t_1$, $t_2$ in Fig. 8)
d) off-state of device

at the beginning (on-state), at $t_1 = 1.03$ µs, at $t_2 = 1.13$ µs and at the end (device in blocking state). This set of EBIC maps is shown in Fig. 9. The images depict the change of the space-charge region during the turn-off process. While the diode is in the on-state (Fig. 9a), the ring-shaped structures are located at the edge of the main p-well (inner ring) and the field ring (outer ring). When the device is turned off and the space-charge region is expanding, as shown in Fig. 9b and Fig. 9c, the electric field at the field-ring is temporarily larger than the field at the p-well. Finally the device is in the off-state, and the electric field of the main p-well is larger compared to the field located at the outer ring. Effects like these will not be visible in the case of stationary measurements and give valuable inputs for an improvement of the edge termination design.

## Low-voltage power MOSFET

**Device Structure.** Another investigated device is a low-voltage power MOSFET employing charge-carrier

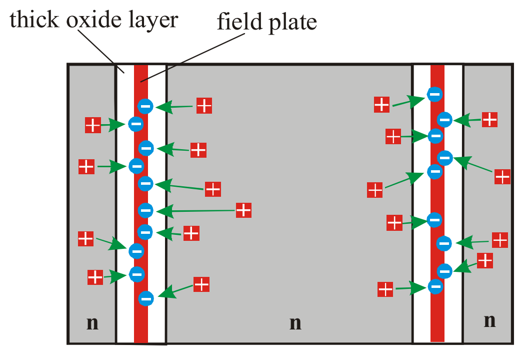


Fig. 10: Compensation of the positive donor charges in the n-region by negative charges located on the field-plates

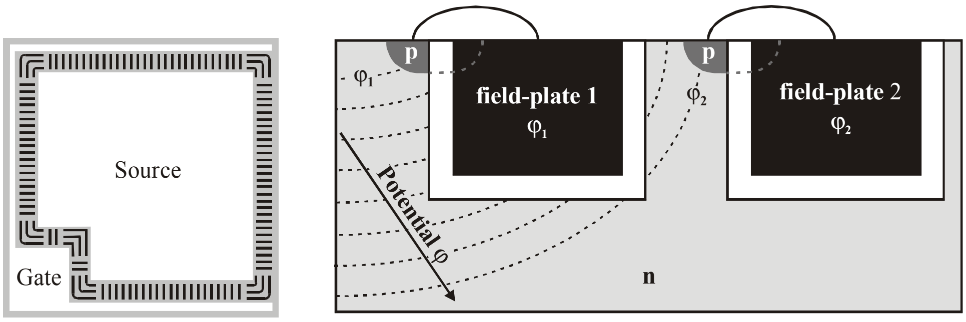


Fig. 11: Schematic drawing of the MOSFET edge termination structure formed by field-plates

compensation by field-plates [10]. Thanks to the compensation principle as depicted in Fig. 10, the specific on-resistance of the device is clearly reduced due to the increased doping density, but the higher doping also requires new edge termination structures.

One proposed termination structure consists of trenches that run radial from the cell array towards the edge region, forming several rings [12]. The trenches are filled with field-plates. Each field-plate is connected to a p-well region which can be reached by the electric field, thus the potential of the field-plate is now set to the potential prevailing in the p-well region as illustrated in Fig. 11.

For a proper operation of the edge-termination structure the field-plate potential must be set to appropriate values, otherwise a premature breakdown occurs. Consequently, an exact positioning of the p-well is essential.

**EBIC Microscopy.** EBIC measurements were employed to identify weak points in the design. In Fig. 12, an inner and an outer corner of the termination structure, which are located between source and gate, are shown in the lower and upper row, respectively. Backscattered electron images indicate the topography of the device surface; EBIC amplitude maps display the strength of measured signals. Since the passivation layer over the U-shaped gate fingers is thinner than on top of the termination structure, more generated electron-hole pairs can be collected. Therefore the EBIC amplitudes created in the gate finger regions must be rescaled when comparing to the EBIC signal on the termination structure.

As the drain-source voltage increases, the way in which the space-charge region distributes across the field-plate rings can be observed. It is obvious that the space-charge region extends only to the first ring and no field is applied to the following rings, except on the corner. With larger applied voltage the EBIC amplitude on the indicated locations increases rapidly, which leads to the situation shown in Fig. 12b. Strong electrical fields in these areas accelerate free excess charge carriers to velocities at which charge multiplication occurs due to

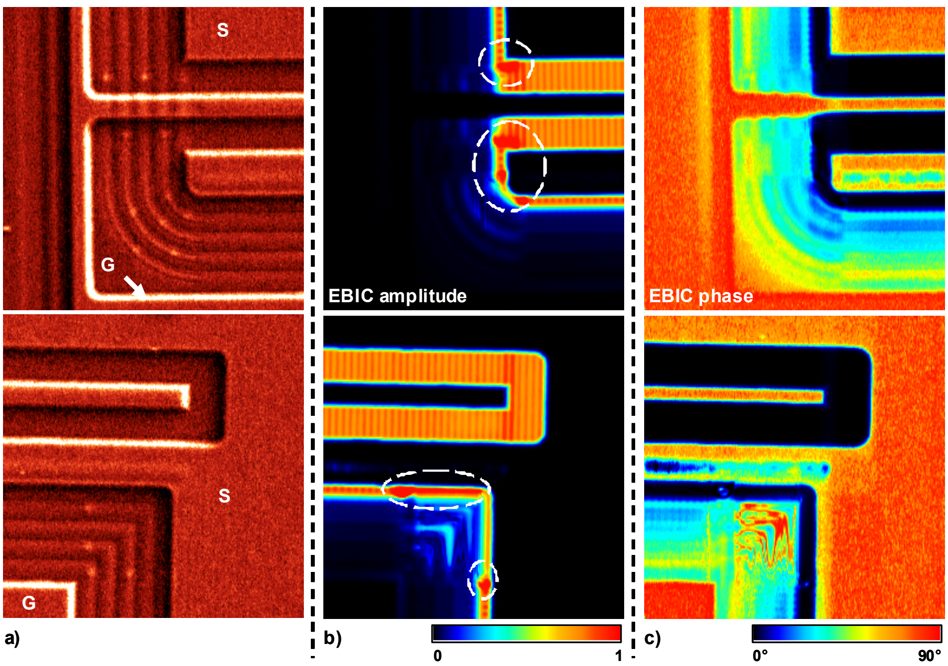


Fig. 12: a) Backscattered electron image of termination structure detail (bright colour: high signal; dark colour: low signal).
b) EBIC amplitude map (normalized scale); circles indicate premature breakdown locations.
c) EBIC phase map from the same region as in (a) (scale in degrees).

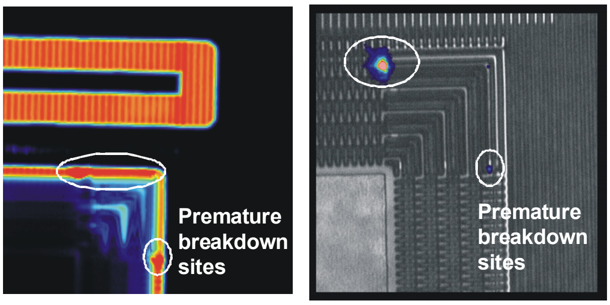


Fig. 13: Comparison of premature breakdown location as found by EBIC measurement (left) and backside emission measurement (right) in the edge termination structure of the MOSFET device

avalanche effect. For accurate determination of the premature breakdown location, the EBIC maps can be overlaid with the backscattered electron maps and the chip layout. The depth at which the electric-field strength reached the maximum value was determined by variation of the primary electron energy, and is equal to the depth of the trench structure.
EBIC Phase maps (Fig. 12c) present the phase shift between the reference signal of the lock-in amplifier and induced currents. It is evident, that the U-shaped gate fingers and the inner field-plate are in phase with the reference. Since no electric field is applied to the other rings, the excess charge carriers diffuse and recombine. Only a small fraction of the free charge carriers reach the space-charge region by diffusion and are collected, therefore the EBIC amplitude is small. Diffusion processes are much slower compared to drift processes, therefore a phase shift is observed.

To test whether the premature breakdown position as indicated in the EBIC maps are reliable, the result was compared with backside emission images on identical structures. An example is given in Fig. 13. Obviously both methods show the same location of the premature breakdown.

While the results and the comparison presented above show in principle the capability of EBIC microscopy to support the analysis of such field-plate structures, there is also a limitation. As a result of electron irradiation, electron-hole pairs are also generated in the insulation layers of the transistor. Due to the much higher mobility of the electrons in silicon oxide, they move out of the insulator and the density of holes increases with time. This leads to a charge imbalance in the silicon oxide [13,14]. Therefore, the electrical properties of the device, especially the electric field distribution, change. Apart from this effect, some positive charge carriers are trapped near the interface of the insulator [15]. The positive charging of the insulator leads to an accumulation of electrons in silicon and the drain-source channel finally becomes conductive. To counter the charging effect in the gate oxide and to be able to apply a blocking voltage between drain and source, a negative voltage has to be connected to the gate. A similar measure is also needed for the field-plate electrode to counterbalance the induced charges in the field insulation - otherwise the maximum blocking voltage of the structure reduces during the measurement.

## CONCLUSION

Ion-beam induced charge (IBIC) microscopy and electron-beam induced charge (EBIC) microscopy were used to study different edge-termination structures of high-power high-voltage diodes and a low-voltage field-plate power MOSFET. Both methods allow the study of the distribution of the electric field and the identification of possible hazardous points in the edge termination design and to identify premature breakdown locations. By employing dynamic measurements it was shown in the case of high-voltage diodes, that the electric field distribution is different under stationary and dynamic conditions. EBIC microscopy offers the advantages of a completely non-destructive measurement and of comparatively easy implementation of the measurement setup since a common electron microscope can be used.

EBIC microscopy is, in principle, a very useful tool for the investigation of field-plate based edge termination structures in power MOSFETs. Nevertheless, the electron beam induces charges in the silicon oxide layers, thus a reduction of the blocking voltage of the entire structure during the measurement occurs if no counter measures are taken.

In comparison to OBIC (Optical Beam Induced Current) microscopy [7,16] both methods allow a depth resolution in the semiconductor volume. On the other hand, the OBIC method has the advantage that it can investigate areas covered by metal layers from the backside of the wafer.

## REFERENCES

[1] Breese, M.B.H, Jamieson, D.N. and. King, P.J.C.: *Materials Analysis using a Nuclear Microprobe*, John Wiley & Sons, 1996

[2] Breese, M.B.H.: A review of ion beam induced charge microscopy for integrated circuit analysis, Materials Science & Engineering, **B42**, 1996, 67-76

[3] Yang, C., Bettiol, A., Jamieson, D., Hua, X., Phang, J.C.H., Chan, D.S.H., Watt, F. and Osipowicz, T.: Investigation of light emitting diodes using nuclear microprobes, Nuclear Instruments and Methods in Physics Research, **B 158**, 1999, 481-486

[4] Osipowicz, T., Sanchez, J.L., Orlic, I., Watt, F., Kolachina, S., Chan, D.S.H. and Phang, J.C.H.: Fluence dependence of IBIC collection efficiency of CMOS transistors, Nuclear Instruments and Methods in Physics Research B, **136**, 1998, 1345-1348

[5] Bogdanovi, I., Fazini, S.; Jaki, M., Vittone, E., and Manfredotti, C.: Nuclear Instruments and Methods in Physics

Research Section B, **130**, 1997, 513-517

[6] Zmeck, M., Balk, L.J., Pugatschow, A., Niedernostheide, F.J., Schulze, H.J., Osipowicz, T., Watt, F., Phang, J.C.H. and Khambadkone, A.M.: Analysis of Premature Breakdown in High-power Devices using IBIC Microscopy, Proc. EPE'05 (Dresden, 2005)

[7] Sandoe, J.N. and Highes, J.R.: EBIC and LBIC techniques for characterization of reverse biased power devices, Acta Electronica, **25**, 1983, .201-209

[8] Raghunathan, R. and Baliga, B.J.: EBIC Investigation of Edge Termination Techniques for Silicon Carbide Power Devices, Proc. ISPSD'96 (Maui, 1996)

[9] Pugatschow, A., Geinzner, T., Heiderhoff, R., Niedernostheide, F. J., Schulze, H.-J., Wiedenhorst, B. and Balk, L.J.: Dynamic Behavior of High-Power Diodes Analyzed by EBIC, Proc. ISPSD'96 (Naples, 2006)

[10] Pawel, I., Siemieniec, R., Roesch, M., Hirler, F., Geissler, C., Pugatschow, A. and Balk, L.J.: Design of Avalanche Capability of Power MOSFETs by Device Simulation, Proc. EPE'07 (Aalborg, 2007)

[11] Zmeck, M., Balk, L.J., Heiderhoff, R., Osipowicz, T., Watt, F., Phang, J.C.H., Khambadkone, A.M., Niedernostheide, F.J. and Schulze, H.J.: Analysis of E-Field Distributions within High-Power Devices Using IBIC Microscopy, Proc. ISPSD'05 (Santa Barbara, 2005)

[12] Hirler, F., Werner, W., Zundel, M. and and Pfirsch, F.: Leistungs-Trenchtransistor, German Patent DE 102004 052678 B3, 2006

[13] Snow, E.H., Grove, A.S. and Fitzgerald, D.J.: Effect of Ionizing Radiation on Oxidized Silicon Surfaces and Planar Devices, Proc. IEEE, **55**, 1967, 1168-1185

[14] Leamy, H.J.: Charge collection scanning electron microscopy, Journal of Applied Physics, **53**, 1982, R51-R80

[15] Woods, M. H. and Williams, R.: Hole traps in silicon dioxide, Journal of Applied Physics, **47**, 1976, 1082-1089

[16] Soelkner, G., Kreutle, J., Quincke, J., Kaindl, W. and Wachutka, G.: "Back side optical beam induced current method for the localization of electric field enhancements in edge termination structures of power semiconductor devices" Microelectronics Reliability, **40**, 2000, 1641-1645

**Addresses of the authors**

Ralf Siemieniec, Infineon Technologies Austria AG, Siemensstr. 2, A-9500 Villach, Austria, e-mail: ralf.siemieniec@infineon.com

Anton Pugatschow, Infineon Technologies Austria AG, Siemensstr. 2, A-9500 Villach, Austria, e-mail: anton.pugatschow@infineon.com

Christian Geissler, Infineon Technologies AG, Wernerwerkstraße 2, D-93049 Regensburg, Germany, e-mail: christian.geissler@infineon.com

Hans-Joachim Schulze, Infineon Technologies AG, Am Campeon 1-12, D-85579 Neubiberg, Germany, e-mail: hans-joachim.schulze@infineon.com

Franz-Josef Niedernostheide, Infineon Technologies AG, Am Campeon 1-12, D-85579 Neubiberg, Germany, e-mail: franz-josef.niedernostheide@infineon.com

Ralf Heiderhoff, Bergische Universität Wuppertal, Rainer-Gruenter-Straße 21, D-42119 Wuppertal, Germany. e-mail: heiderho@uni-wuppertal.de

Ludwig Josef Balk, Bergische Universität Wuppertal, Rainer-Gruenter-Straße 21, D-42119 Wuppertal, Germany, e-mail: balk@uni-wuppertal.de